

Synthesis of Hydrophobic Carbohydrate Polymers and Their Formation of Thermotropic Liquid Crystalline Phases

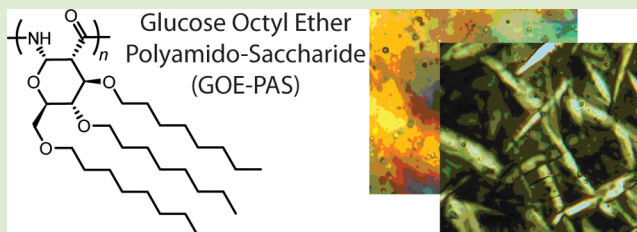
Cynthia Ghobril,[†] Benoît Heinrich,[‡] Eric L. Dane,[†] and Mark W. Grinstaff^{*,†}

[†]Departments of Chemistry and Biomedical Engineering, Boston University, Boston, Massachusetts 02215, United States

[‡]Institut de Physique et Chimie des Matériaux de Strasbourg, UMR CNRS Uds 7504, 23 rue du Loess, BP 43, 67034 Strasbourg Cedex 2, France

S Supporting Information

ABSTRACT: The first synthesis of enantiopure glucose octyl ether polyamido-saccharides (GOE-PAS) with a defined molecular weight and narrow dispersity is reported using a controlled anionic ring-opening polymerization of a glucose-derived β -lactam sugar monomer possessing octyl ether chains. This new polymer structure is characterized by NMR, infrared (IR), optical rotation, gel permeation chromatography (GPC), and thermogravimetric analysis (TGA). At room temperature, the polymers form lamellar (Lam) phases. Upon heating to mild temperatures (ca. 60 °C), the shortest polymer shows a direct transition to the isotropic (Iso) liquid state, while the longer polymers give rise to a hexagonal columnar (Col_h) phase before becoming isotropic at higher temperatures (ca. 120 °C).



The preparation of novel synthetic polymers that possess well-defined, complex repeat unit structures and the study of how structural variables in the repeat unit influence materials properties are of interest from both fundamental and applied perspectives. Natural biopolymers represent a rich source of inspiration for new synthetic polymers, such as poly(β -peptides),¹ polypeptoids,² poly(α -hydroxyacids),³ and others.⁴ In particular, polysaccharides are of interest because they contain a large number of stereocenters, a backbone that is rigidified by the presence of a pyranose ring, and a range of linkage geometries.⁵ Hence, the number of structural variables that can be tuned by synthesis is large.⁶ Studies on natural and derivatized polysaccharides have shown the importance of these structural parameters in determining materials properties.⁷ However, such polymers are challenging to access synthetically from the monomer level because of the high density of similar functional groups found on polysaccharides and the need to control the configuration of the glycosidic linkage.⁸ In response to the need for methods to prepare synthetic polymers that capture many of the unique and desirable properties of natural polysaccharides, we have recently reported a synthetic approach that replaces the ether linkage found in natural polysaccharides with an amide linkage and named these polymers polyamido-saccharides (PASs).⁹ Our approach is notable for allowing the preparation of enantiopure carbohydrate polymers of low polydispersity (\mathcal{D}) and controlled molecular weight. Herein, we extend the methodology to the synthesis of glucose octyl ether polyamido-saccharides (GOE-PASs), specifically α -N-1,2-D-glucose octyl ether PASs, with molecular weights as high as 50 kDa. The substitution of the glucose-derived repeat unit with three octyl chains results in hydrophobic polymers with

liquid crystalline phases at room temperature and up to 120 °C (Figure 1).

Liquid crystalline (LC) materials feature mesophases with a physical behavior intermediate between the solid and the liquid state. In LC phases, molecules retain varying degrees of the long-range order found in crystalline solids while having some of the translational freedom characteristic of liquids. Small molecule liquid crystals are widely used in display technologies because of their ability to modulate the transmission of polarized light under the influence of an electric field.¹⁰ Understanding how LC properties observed in small molecules can be translated to polymeric systems is an area of great interest as the ability to form polymer films with supramolecular order is essential to engineering complex functional materials.¹¹ It is known that certain polysaccharides, with their rigidified, rod-like backbone, can form LC phases in bulk and in solution.¹² For example, cellulose derivatives have been reported to form both lyotropic and thermotropic LC phases, with chiral nematic phases being most commonly observed.¹³ In thermotropic LC phases, flexible molecular segments that melt at elevated temperatures, such as aliphatic chains, act as a solvent. In the absence of a molten phase, polysaccharides are either amorphous or semicrystalline materials with glass transitions and melting points that are generally above their decomposition temperature. In our PAS system, the octyl ether chains act as a molten phase and allow the rod-like carbohydrate backbone to assemble first into a lamellar LC phase and then into a hexagonal columnar LC phase.

Received: February 3, 2014

Accepted: March 19, 2014

Published: March 27, 2014

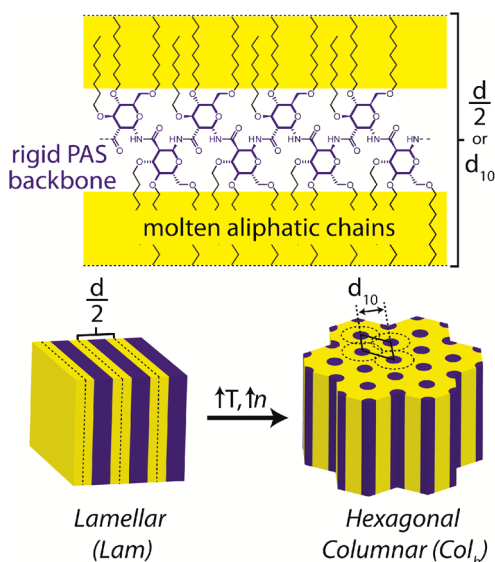
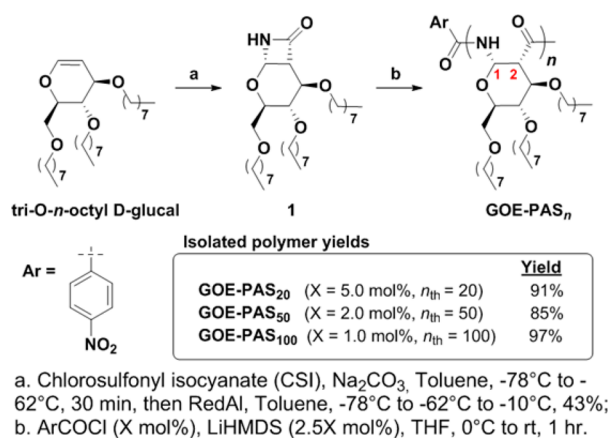


Figure 1. Graphical representation of the structural packing of GOE-PAS_n in the lamellar (Lam) and hexagonal columnar (Col_h) mesophases. $d/2$: the position of the main reflection and thickness of a single layer in the Lam phase. d_{10} : the position of the first-order reflection of the 2D lattice in the Col_h phase. T : temperature. n : number of monomer repeat units.

The synthesis of GOE-PAS of different theoretical degrees of polymerization (DP_{th}), GOE-PAS₂₀, GOE-PAS₅₀, and GOE-PAS₁₀₀ (DP_{th} = 20, 50, 100, respectively), is shown in Scheme 1. The glucose-derived β -lactam monomer **1** was obtained in

Scheme 1. Polymer Synthesis



moderate yield from the stereoselective cycloaddition of tri-O-octyl-D-glucal¹⁴ and chlorosulfonyl isocyanate (CSI) followed by the reductive removal of the sulfonyl group.¹⁵ *Para*-nitrobenzoyl chloride was used as the initiator for the anionic

ring-opening polymerization of monomer **1** which was performed at three different initiator loadings (5, 2, and 1 mol %), allowing the preparation of GOE-PAS_n with variable molecular weights.⁹ The polymers were obtained as pasty solids and were characterized by ¹H and ¹³C NMR spectroscopy, gel permeation chromatography (GPC), polarimetry, infrared (IR), and thermogravimetric analysis (TGA) (see Supporting Information (SI)). The ¹H NMR spectra for all three polymer lengths showed the peaks expected for the proposed structure, with the peaks being somewhat broadened as commonly observed for polymeric structures. The end group proton signals were visible at 8.1–8.3 ppm and decreased in comparison to repeat unit signals with increasing molecular weight, as expected. The DP_{NMR} was estimated by comparing the integration of the end group's aromatic signal at 8.3 ppm to the polymer integration at 0.88 ppm (terminal methyl groups of the octyl chains) (Table 1). The ¹³C NMR spectra also confirmed the proposed structure, showing all expected signals, notably those at 171 ppm (amide), 76 ppm (C1), and 51 ppm (C2). Polymer molecular weights were determined using GPC (THF) with polystyrene standards (Table 1). The GOE-PAS_n M_n values were in good agreement with theory. The measured dispersities (\bar{D}) were low (1.1), as was previously found with the benzyl-substituted glucose and galactose-derived PASs.^{7,14} The specific rotations of GOE-PAS_n were measured in CHCl₃ at 26.7 °C ($[\alpha]_D = 77.9$ (GOE-PAS₂₀), 84.5 (GOE-PAS₅₀), 80.6 (GOE-PAS₁₀₀)). The IR spectra of GOE-PAS_n show strong amide (amide I ≈ 1685 cm⁻¹ and amide II ≈ 1528 cm⁻¹) and C–H (≈ 2800 –3000 cm⁻¹) stretches. By TGA, the polymers are stable up to 200 °C (see SI, Figure S1).

The thermotropic LC properties of GOE-PAS_n were investigated by polarizing optical microscopy (POM), differential scanning calorimetry (DSC), and small-angle X-ray scattering (SAXS). Birefringent and pasty POM textures were obtained in the pristine state for the three GOE-PAS polymers, which is indicative of a native mesophase organization (Figure 2 and SI, Figure S2). Further fluidizing with the preservation of

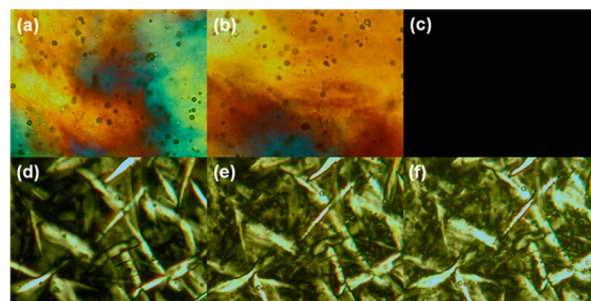


Figure 2. POM textures of GOE-PAS₅₀ at rt (a); upon heating to 90 °C (b) and to 120 °C in the Iso phase (c); and upon cooling from the Iso phase to 90 °C (d), to 60 °C (e), and to rt (f). Image exposure times upon heating and cooling are identical.

Table 1. Polymer Characterization

	$M_{n(th)}$ (kDa)	$M_{n(NMR)}^a$ (kDa)	$M_{n(GPC)}^b$ (kDa)	$M_{w(GPC)}^b$ (kDa)	\bar{D}^c	DP _{th}	DP _{NMR} ^a	DP _{GPC} ^b	$[\alpha]_D$ (CHCl ₃) ^d
GOE-PAS ₂₀	10.7	13.3	11.3	12.1	1.1	20	25	21	+77.9
GOE-PAS ₅₀	26.4	31.7	26.3	27.7	1.1	50	60	50	+84.5
GOE-PAS ₁₀₀	52.8	59.1	47.4	51.4	1.1	100	112	90	+80.6

^aDetermined by integration of the ¹H NMR signal from the aromatic group on the initiator. ^bTHF GPC with polystyrene standards. ^c $\bar{D} = M_w/M_n$. ^d[GOE-PAS₂₀] = 5.04 mg/mL, [GOE-PAS₅₀] = 5.13 mg/mL, [GOE-PAS₁₀₀] = 4.79 mg/mL, $T = 26.7$ °C.

birefringence is observed upon heating until the transition to the isotropic phase is reached, at around 60 °C for GOE-PAS₂₀ and 120 °C for GOE-PAS_{50/100}. GOE-PAS₂₀ remains isotropic upon cooling to room temperature, whereas the liquid crystalline state of the two longer polymers is restored with a few degrees of hysteresis. Textures with large defects could be grown for phase identification and stayed unmodified upon further cooling, indicating that no phase transition was crossed. However, an unambiguous identification of the nature of the mesophase from POM textures was not possible, as is sometimes the case with polymeric mesogens.¹⁶

By DSC, GOE-PAS₂₀ shows an endothermic transition at 50 °C on first heating that can be easily related to the isotropization recorded in POM (Figure 3). GOE-PAS₅₀ and

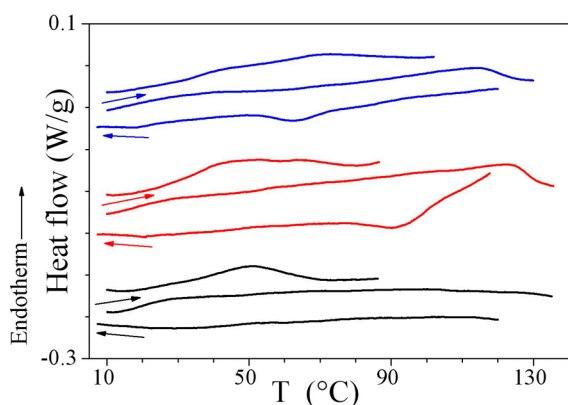


Figure 3. DSC thermograms of GOE-PAS₂₀ (bottom, black), GOE-PAS₅₀ (middle, red), and GOE-PAS₁₀₀ (top, blue). GOE-PAS₂₀: first heating run with endothermic transition at 50 °C (top line); second heating run (middle) and cooling run (bottom) with no reverse transition observed upon cooling. GOE-PAS_{50/100}: first heating run with endothermic transitions at 45 and 65 °C, respectively (top line); second heating run with phase transition at 110–130 °C (middle); second cooling run with reverse-phase transition below 100 °C (bottom). Heating and cooling ramps: 10 °C/min.

GOE-PAS₁₀₀ show an endothermic transition at 45 and 65 °C, respectively, before becoming isotropic between 110 and 130 °C, as recorded by POM (Figure 3). These transitions are associated with small enthalpy changes, in the range of 1–2 J/g, which is indicative of mesophases with a low degree of translational order and consistent with the highly fluid textures

above room temperature. Upon the second cooling, no reverse-phase transition of GOE-PAS₂₀ is observed by DSC. The longer polymers, GOE-PAS_{50/100}, on the other hand, show a reverse-phase transition below 100 °C. A subtle change in the slope of the DSC curve, which corresponds to the glass transition, occurs in the region of 15–25 °C for the two longer polymers. In comparison to small molecule mesogens, polymers often show broadened phase transitions that extend over a large range of temperatures.¹⁶ In regard to polymeric systems, it has been shown, for example, that in LC tri-*O*-heptyl cellulose (THC) both the temperature and the broadness of the transition to Iso are dependent on the molecular weight of the polymer.¹⁷ Specifically, lower molecular weight THC polymers (5–30 kDa) displayed transitions to the Iso phase that were broadened, of lesser enthalpy, and at a lower temperature in comparison to higher molecular weight THC polymers (300–500 kDa). Thus, the broadened transitions observed by DSC for GOE-PASs are a consequence of their polymeric structure and, more specifically, may be related to the molecular weight range (10–50 kDa) that was investigated, as studies on THC have shown this molecular weight range to display broadened transitions relative to longer polymers.

Additional studies by SAXS allowed the identification of the nature of the mesophases. The X-ray diffraction pattern of GOE-PAS₂₀ displays, at room temperature, a lamellar (Lam) mesophase with a set of four reflections in the low-angle region, with reciprocal spacings in the ratio 1:2:3:4, assigned to the first, second, third, and fourth lamellar order reflections (Figures 1 and 4a). On the basis of the high intensity of the second-order reflection and the analysis of the molecular structure, $d/2$ represents the thickness of a single layer in the Lam phase (Figures 1 and 4a). Pristine GOE-PAS₅₀ and GOE-PAS₁₀₀ also show a Lam mesophase with additional reflections indicative of another coexisting mesophase (Figures 1 and 4b,c). The broad scattering maximum near $2\theta = 20^\circ$ (approximately 4.5 Å) results from lateral spacings of the aliphatic chains (h_{ch}) and, presumably, from a contribution of the short-range correlated periodicity along the polymer backbone (h_{GLA}) (Figure 4).¹⁸ Polymer GOE-PAS₂₀ exhibits the closest spacing between lamellar layers $d/2$ (21.5 Å) (see SI, Figure S3 at 20 °C). Increasing polymer length results in lamellar spacing of 22.0 Å for GOE-PAS₅₀ and 22.5 Å for GOE-PAS₁₀₀. The increase in lamellar spacing with polymer length can be understood as resulting from the aliphatic chains being forced into a more extended conformation as the rod-like cores

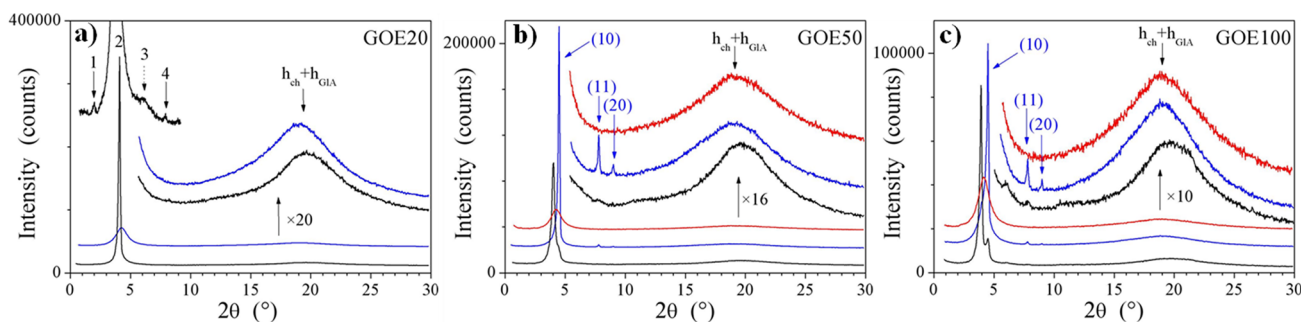


Figure 4. X-ray diffractograms of GOE-PAS_n in the pristine state at room temperature (black), at 80 °C (blue, Iso for GOE-PAS₂₀ and Col_h for GOE-PAS_{50/100}), and at 120 °C (red, Iso for GOE-PAS_{50/100}). Patterns with offset (below), expansion of WAXS range (above); (a) SAXS pattern in the pristine state at room temperature (top, left, black), where the reflections 1, 2, 3, and 4 are lamellar orders; (b,c) (10), (11), and (20) are the reflections of the bidimensional hexagonal lattice; h_{ch} and h_{GLA} are diffuse scatterings due to lateral distances between aliphatic chains and, presumably, to periodicities along the polymer core.

of the longer polymers pack more closely. This effect is also shown in the decrease in molecular area (S_{Lam}), which is the statistical layer portion covered by a single repeat unit, with increasing molecular weight (see SI, Figure S3).¹⁹

Upon heating to 80 °C, GOE-PAS₂₀ displays an isotropic phase (Figure 4a, blue), whereas GOE-PAS₅₀ and GOE-PAS₁₀₀ show another mesophase (Figure 4b,c, blue), delaying the transition to the isotropic liquid to higher temperatures (Figure 4b,c, red). The X-ray diffraction patterns in this intermediate mesophase display a set of three small-angle reflections, with reciprocal spacings in the squared ratio 1:3:4, assigned to (10), (11), and (20) reflections of a bidimensional hexagonal lattice (Figure 4b,c). Thus, this phase is a hexagonal columnar mesophase (Col_h) formed by the parallel alignment of the individual polymer backbones separated from each other by a continuum of molten aliphatic chains (Figure 1). Due to the homogeneous distribution of the aliphatic periphery, the distance between adjacent polymer rows, d_{10} , equal to 19.5 Å, is smaller than the layer thickness $d/2$ in the Lam phase (see SI, Figure S3). As expected, the identical repeat unit structures lead to similar geometrical parameters for both of the longer polymers (see SI, Figure S3). The absence of a Col_h phase for GOE-PAS₂₀ is presumably due to its lower aspect ratio (close to 3.3) compared to the longer polymers.²⁰ Thus, GOE-PAS₂₀ has a less elongated rod-like shape that is not as favorable for the parallel alignment of backbones defining the common direction of the columnar axis in the mesophase.

In comparison to natural polysaccharides in which the hydroxyl groups are substituted with long-chain alkyl groups, the self-assembling properties of GOE-PAS polymers show both similarities and notable differences. For example, tri-*O*-alkyl ether cellulose polymers are reported to form both thermotropic and lyotropic LC phases depending on the length of the alkyl chain. Specifically, the tri-*O*-octyl ether cellulose is described as a gummy solid that formed lyotropic cholesteric phases in chloroform, and the formation of a thermotropic LC phase is not observed.²¹ For long-chain ester derivatives of cellulose, thermotropic LC behavior is reported for polymers derivatized with alkyl chains of eight or more carbons, with the main LC phase identified as hexagonal columnar.¹⁸ Thus, we find that the derivatization of PAS polymers with long-chain octyl groups promotes LC formation, in agreement with earlier studies. However, in contrast to cellulose derivatives, GOE-PAS polymers already display mesophases at room temperature and up to 120 °C (as compared to >80 °C in the tri-*O*-alkyl ester cellulose series). This presumably reflects differences in the backbone's conformation and rigidity of the polymers.

In summary, the synthesis of enantiopure glucose octyl ether polyamido-saccharides with controlled molecular weight and narrow dispersity is reported. The polymers are characterized using NMR spectroscopy, optical rotation, IR, GPC, and TGA. On the basis of POM, DSC, and SAXS, in the pristine state, the polymers are found to be thermotropic liquid crystals that form lamellar and hexagonal columnar mesophases depending on the temperature and the polymer chain length. This study highlights how the amide-linked carbohydrate-derived PAS structure can be used as a well-defined, rigid-rod backbone to form polymers that assemble into mesophases. The ease of monomer and polymer synthesis combined with the control over molecular weight and dispersity provided by the method suggest that a range of LC materials can be prepared using our approach. Ongoing work is focused on investigating the

backbone conformation as well as the effect of configuration, alkyl chain length, and branching on supramolecular assembly.

■ ASSOCIATED CONTENT

■ Supporting Information

Experimental details and ¹H and ¹³C NMR spectra, TGA, SAXS interpretation and POM. This material is available free of charge via the Internet at <http://pubs.acs.org>.

■ AUTHOR INFORMATION

Corresponding Author

*E-mail: mgrin@bu.edu.

Notes

The authors declare no competing financial interest.

■ ACKNOWLEDGMENTS

We thank BU for support of this research, and E.L.D. acknowledges receipt of an NIH/NIGMS Postdoctoral Fellowship (1F32GM097781).

■ REFERENCES

- (1) (a) Seebach, D.; Gardiner, J. *Acc. Chem. Res.* **2008**, *41*, 1366. (b) Horne, W. S.; Gellman, S. H. *Acc. Chem. Res.* **2008**, *41*, 1399. (c) Cheng, R. P.; Gellman, S. H.; DeGrado, W. F. *Chem. Rev.* **2001**, *101*, 3219.
- (2) Sun, J.; Zuckermann, R. N. *ACS Nano* **2013**, *7*, 4715.
- (3) Lu, Y.; Yin, L.; Zhang, Y.; Xu, Y.; Tong, R.; Cheng, J. *ACS Macro Lett.* **2012**, *1*, 441.
- (4) (a) Zhang, H.; Grinstaff, M. W. *J. Am. Chem. Soc.* **2013**, *135*, 6806. (b) Aida, T.; Meijer, E. W.; Stupp, S. I. *Science* **2012**, *335*, 813. (c) Deming, T. J. *Top. Curr. Chem.* **2012**, *310*, 1. (d) Ray, W. C.; Grinstaff, M. W. *Macromolecules* **2003**, *36*, 3557. (e) Hill, D. J.; Mio, M. J.; Prince, R. B.; Hughes, T. S.; Moore, J. S. *Chem. Rev.* **2001**, *101*, 3893.
- (5) (a) Wathier, M.; Lakin, B. A.; Bansal, P. N.; Stoddart, S.; Snyder, B. D.; Grinstaff, M. W. *J. Am. Chem. Soc.* **2013**, *135*, 4930. (b) Mikami, K.; Lonnet, A. T.; Gustafson, T. P.; Zinnel, N. F.; Pai, P.-J.; Russell, D. H.; Wooley, K. L. *J. Am. Chem. Soc.* **2013**, *135*, 6826. (c) Bonduelle, C.; Lecommandoux, S. *Biomacromolecules* **2013**, *14*, 2973. (d) Liao, S. W.; Yu, T.-B.; Guan, Z. *J. Am. Chem. Soc.* **2009**, *131*, 17638.
- (6) Tirelli, N. *Macromol. Biosci.* **2006**, *6*, 575.
- (7) (a) Crouzier, T.; Boudou, T.; Picart, C. *Curr. Opin. Colloid Interface Sci.* **2010**, *15*, 417. (b) Malafaya, P. B.; Silva, G. A.; Reis, R. L. *Adv. Drug Delivery Rev.* **2007**, *59*, 207.
- (8) Gruner, S. A. W.; Locardi, E.; Lohof, E.; Kessler, H. *Chem. Rev.* **2002**, *102*, 491.
- (9) (a) Dane, E. L.; Chin, S. L.; Grinstaff, M. W. *ACS Macro Lett.* **2013**, *2*, 887. (b) Dane, E. L.; Grinstaff, M. W. *J. Am. Chem. Soc.* **2012**, *134*, 16255.
- (10) (a) Demus, D.; Goodby, J.; Gray, G.; Spiess, H.; Vill, V. *Handbook of Liquid Crystals*; Wiley-VCH: Weinheim, Germany, 1998; p 731. (b) Bahadur, B. (Ed.) *Liquid Crystals: Application and Uses*; World scientific: Singapore, 1990–92.
- (11) (a) Pomerantz, W. C.; Yuwono, V. M.; Drake, R.; Hartgerink, J. D.; Abbott, N. L.; Gellman, S. H. *J. Am. Chem. Soc.* **2011**, *133*, 13604. (b) Hamley, I. W. *Soft Matter* **2010**, *6*, 1863. (c) Yang, S.-H.; Hsu, C.-S. *J. Polym. Sci., Part A: Polym. Chem.* **2009**, *47*, 2713. (d) Donnio, B.; Buathong, S.; Bury, I.; Guillon, D. *Chem. Soc. Rev.* **2007**, *36*, 1495. (e) Li, M.-H.; Keller, P. *Phil. Trans. R. Soc. A* **2006**, *364*, 2763.
- (12) Fukuda, T.; Tsujii, Y.; Miyamoto, T. *Macromol. Symp.* **1995**, *99*, 257.
- (13) Gray, D. G. *Carbohydr. Polym.* **1994**, *25*, 277 and references herein.
- (14) Vedachalam, S.; Tan, S. M.; Teo, H. P.; Cai, S.; Liu, X.-M. *Org. Lett.* **2012**, *14*, 174. Procedure modified by using 1-iodooctane instead of 1-bromooctane.

- (15) Kaluža, Z.; Abramski, W.; Bełzecki, C.; Grodner, J.; Mostowicz, D.; Urbański, R.; Chmielewski, M. *Synlett* **1994**, 539.
- (16) Lenz, R. W. *Pure Appl. Chem.* **1985**, 57, 977.
- (17) Takada, A.; Fukuda, T.; Watanabe, J.; Miyamoto, T. *Macromolecules* **1995**, 28, 3394.
- (18) Yamagishi, T.; Fukuda, T.; Miyamoto, T.; Takashina, Y.; Yakoh, Y.; Watanabe, J. *Liq. Cryst.* **1991**, 10, 467.
- (19) $S_{\text{Lam}} = V_{\text{Mol}}/(d/2)$: molecular area of a single repeat unit in the Lam phase, where $V_{\text{Mol}} = 880 \text{ \AA}^3$ is the repeat unit volume at 20 °C, evaluated from single-crystal structures of the Cambridge database (structure JIJXIJ) and from reference density measurements. See formulas in: de Gracia Lux, C.; Donnio, B.; Heinrich, B.; Krafft, M.-P. *Langmuir* **2013**, 29, 5325.
- (20) $AR = L/D$: aspect ratio of the cylinders of diameters D , with the same lengths L and volumes V_c as the polymer backbones. $D = (4/\pi x_{V_c} A_{\text{Col}})^{0.5} = 12.1 \text{ \AA}$, where $x_{V_c} = 0.261$ is the volume fraction of the polymer backbones and $A_{\text{col}} = 440 \text{ \AA}^2$ is the lattice area; $L = nV_{\text{Mol}}/A_{\text{Col}}$, where $V_{\text{Mol}} = 880 \text{ \AA}^3$ is the repeat unit volume and n is the polymerization degree. (GEO-PAS₂₀: $L = 40 \text{ \AA}$, $AR \approx 3.3$; GEO-PAS₅₀: $L = 100 \text{ \AA}$, $AR \approx 8.3$; GEO-PAS₁₀₀: $L = 200 \text{ \AA}$, $AR \approx 16.5$).
- (21) Isogai, A.; Ishizu, A.; Nakano, J. *J. Appl. Polym. Sci.* **1986**, 31, 341.